2018-04-10

Marrow-Isolated Adult Multilineage Inducible (MIAMI) and Annulus Fibrosus Cell Co-Cultures on Electrospun Polycaprolactone Scaffolds for Intervertebral Disc Tissue Engineering

Flavia Zisi Tegou
University of Miami, flaviategou@gmail.com

UNIVERSITY OF MIAMI

MARROW-ISOLATED ADULT MULTILINEAGE INDUCIBLE (MIAMI) AND ANNULUS FIBROSUS CELL CO-CULTURES ON ELECTROSPUN POLYCAPROLACTONE SCAFFOLDS FOR INTERVERTEBRAL DISC TISSUE ENGINEERING

By

Flavia Zisi Tegou

A THESIS

Submitted to the Faculty
of the University of Miami
in the partial fulfillment of the requirements for
the degree of Master of Science

Coral Gables, Florida

May 2018

UNIVERSITY OF MIAMI

A thesis submitted in partial fulfillment of
the requirements for the degree of
Master of Science

MARROW-ISOLATED ADULT MULTILINEAGE INDUCIBLE (MIAMI) AND ANNULUS FIBROSUS CELL CO-CULTURES ON ELECTROSPUN POLYCAPROLACTONE SCAFFOLDS FOR INTERVERTEBRAL DISC TISSUE ENGINEERING

Flavia Zisi Tegou

Approved:

_____ Fotios Andreopoulos, Ph.D. Associate Professor of Biomedical Engineering	_____ Alicia Jackson, Ph.D. Assistant Professor of Biomedical Engineering
_____ Gianluca D'Ippolito, Ph.D. Lecturer of Biomedical Engineering	_____ Guillermo Prado, Ph.D. Dean of the Graduate School

ZISI TEGOU, FLAVIA (M.S, Biomedical Engineering)
Marrow-Isolated Adult Multilineage Inducible (MIAMI) and Annulus Fibrosus Cell Co-Cultures on Electrospun, Polycaprolactone Scaffolds for Intervertebral Disc Tissue Engineering. (May 2018)

Abstract of a thesis at University of Miami.

Thesis supervised by Professor Fotios Andreopoulos
No. of pages in text (52).

Back pain affects more than 80% of the adult population between the ages of 45-54 years old, and it is a leading cause of disabilities in developing countries. For the most part, low back pain is associated with degeneration of the intervertebral disc (IVD) called degenerative disc disorder (DDD) or degenerative IVD disorder (IDD). Current treatment options are all symptomatic and lead to further degeneration of adjacent vertebrae. Although tissue engineering approaches show potential for treatment of DDD, IVD cells are not readily available, rendering their use for implantation difficult. This study focuses on the use of marrow-isolated adult multilineage inducible (MIAMI) cells co-cultured together with native annulus fibrosus (AF) cells as alternative source for IVD tissue engineering. Moreover, the paper proposes the use of electrospun, polycaprolactone (PCL) scaffolds as substrates for the culture of the cells. The hypothesis was that co-culturing AF and MIAMI cells on PCL scaffolds would lead to differentiation of the latter ones into native disc lineages effectively. PCL scaffolds with random fiber orientation were fabricated using different solvents (DCM and HFIP) and polymer concentrations (12%, 15% and 20%). Scaffolds were characterized using scanning electron microscopy (SEM) for their fiber diameter and uniformity. PCL/HFIP constructs possessed superior properties, with uniform fibers and diameters of 0.88±0.27, 0.94±0.35, and 2.07±0.18μm for 12%, 15% and 20% scaffolds respectively. Porcine AF and MIAMI cells were obtained

and co-cultured on scaffolds for 1, 2 and 3 weeks, by which time samples were obtained for RT-PCR. Cells were tested for the expression of markers *Col I, II, Acan,* as well as *Oct-4* and *Nanog*. AF cells alone were also seeded on tissue culture plates and their ability to differentiate into osteogenic lineages was studied through the addition of osteogenic media. Cells on the scaffolds did not yield consistent Ct values after PCR, however, co-cultured cells seeded on scaffolds for three weeks had distinct expression of *Col 1* and *Acan,* with a significant increase of *Col 1* compared to MIAMI-only controls. AF that underwent osteogenesis tested positive for osteogenic markers *Alk-P, Osteocalcin* and *Osterix* unlike the AF controls (normal culture), which tested negative.

TABLE OF CONTENTS

LIST OF FIGURES

LIST OF TABLES

CHAPTER 1: INTRODUCTION

1.1 Intervertebral disc (IVD) Anatomy and Physiology

IVDs lie between the vertebral bodies of the spine and have an essential role in the mechanics of the spine, as they bare the load of the body weight and muscle activity and resist compression of the spine[1-4]. The mechanical properties of the discs allow for flexibility and extension of the spine, due to the spreading of the loading forces evenly around the vertebral bodies[1-4]. With a varying height of 7-10mm and a diameter of approximately 4cm, the discs are constituting for one third of the spinal height[1]. Their complex structure results from three distinct components: the annulus fibrosus, the nucleus pulposus and the endplates[1-4]. The AF is the outer section of the discs and consists of rings of fibrous cartilage, while the NP is in the center of the AF and is more gelatinous-like[1,3]. The endplates are located in the upper and lower boundaries between the disc and the vertebral bodies, and are cartilaginous[1,3]. The AF is the outer ring of the disc, containing 15-25 concentric lamellae each separated with a layer of primarily collagen I fibers[1,2]. The cells that reside in the AF are fibroblast-like and tend to lie between the outer and inner portion of the structure[1,3]. Particularly, on the outer part of the ring, the cells are thin, elongated and follow the alignment of the collagen fibers; moving towards the inner area of the AF the cells tend to be more oval-shaped[1,3]. The NP contains collagen II and elastin fibers, with a more random organization compared to the fibers in the AF[1,3]. The cells on this portion are chondrocyte-like and have a lower cell density[1-3]. Collagen II and proteoglycan production in the NP is a result of hydrostatic pressure applied on the NP portion[1]. As shown in different studies, the two main macromolecules of the IVD are collagen and proteoglycans (particularly aggrecan), which compose the extracellular

matrix (ECM) of the disc, providing its anchoring and tensile strength[1-3]. Aggrecan, the major proteoglycan of the IVD, is responsible for the tissue hydration and ability of tissue to resist compression and is highly concentrated at the NP analogue[1-4]. Thus, the water content in the nucleus pulposus is elevated, making the tissue act like a shock absorber[1-4]. AF has two main functions; it provides elasticity and motion of the spine, and contains nuclear pressure resulting from the compression of the NP analogue[5]. These characteristics of the disc enable high anisotropic properties, which are crucial to withstand the forces of the spine[5].

1.2 IVD Degeneration Pathophysiology

Back pain is a common, major experience impacting approximately 80% of the population around the world, greatly reducing quality of life and being a leading cause of disability in developed countries for people between 45-54 years[3,4]. Together with other clinical symptoms, chronic low back pain is associated with degeneration of the intervertebral disc (IVD) called degenerative disc disorder (DDD) or degenerative IVD disorder (IDD). During IVD degeneration, the extracellular matrix (ECM) composition, as well as the water content are progressively altered, thus modifying the disc's mechanical properties[6]. Structurally, DDD can result from tears in the annulus fibrosus, disc prolapse, internal disc disruption and end-plate damage[2]. Tears in the AF can be circumferential, radial or peripheral, depending on the location of the damage[2]. Disc prolapse is the condition where the NP migrates into the annular lamellae, while internal disc disruption is the opposite; mainly the collapse of the inner AF portion into the nucleus pulposus, which is usually the aftermath of an end-plate damage[2]. During end-plate damage, the NP, which normally acts like a shock absorber, decompresses, transferring the loads of the

vertebrae into the AF that, as a result, collapses back into the nucleus[2]. Altogether, the main characteristics of the DDD involve decrease in the cell component, proteoglycan breakdown and loss of water content abilities of the NP[2].

1.3 Current Therapeutic Approaches and Tissue Engineering Solutions

During disc degeneration, the structure and biochemical aspects of the IVD are altered, which leads to a great amount of pain and discomfort, and modifies the mechanics of the spine, leading to other severe symptoms, like spondylosis[7]. Current treatments on the market used for the confrontation of DDD are symptomatic rather than curative and range between mitigation therapies and surgical intervention (discectomy or spinal fusion) depending on the severity of the condition[8-11]. Focused more on treating the symptoms rather than the degeneration of the disc itself, none of these techniques have effective, long-term results and usually require taking further measures in the future[8-11]. Particularly, discectomy and spinal fusion are proven to alter the biomechanics of the spine and lead to degeneration of adjacent vertebrae[8-11]. In the recent years, attempts for total disc arthroplasty (as a method to maintain segmental motion of the spine) have been approved, however, due to mechanical wear, the long-term success of the constructs is questionable[12,13]. Hence the establishment of a more effective technique is pivotal.

Tissue engineering has immersed the past years as a new, promising option for IVD degeneration treatment[7-14]. Tissue engineering utilizes and combines cells and scaffolds, with different morphologies and properties to create viable tissues with characteristics similar to the native ones[14]. Generally, scaffolds play an essential role in tissue engineering, by providing an environment for the expression of appropriate ECM and the support of the growth, proliferation and proper function of cells[8,10]. Other than the biochemical properties,

scaffolds provide mechanical support in the tissue, which is something crucial when designing constructs for implantation[8]. Ideally, for an IVD replacement, the constructs must be able to sustain the appropriate cell types and ECM, be porous to provide the necessary transport of waste and nutrients, mimic the mechanical characteristics of the native disc and finally be biocompatible, to allow for implantation *in vivo* without creating adverse effects on the host[8].

Regarding the field of IVD tissue engineering, great advances have marked the past years, through the development of novel approaches to cell culturing and scaffolding. Researchers have managed to approach the DDD through intervention and control of the degeneration through cell culturing in presence or absence of scaffolds[15-16]. Three are the distinct approach attempts to the issue: molecular therapies (utilizing growth factors and gene therapy), cell therapy, and tissue engineering based on biomaterials[17-24]. Disc degeneration was thought, initially, to only have its origins on NP, due to the fact that loss of the proteoglycan and water content yielded a decreased shock absorber ability[25]. With that in mind it is easy to understand why most of the tissue engineering research has been mainly focused on the NP part of the disc, trying to mimic its ECM components and deal with restoring the compression ability. However, although researchers were able to create *in vitro* models biomimetic to the NP and able to restore the disc height, most of these approaches are neither efficacious nor feasible for implantation, since they lack an outer AF portion to maintain the tension of the constructs [7,11,16,26].

Research involving the AF portion of the disc has been utilizing techniques like electrospinning and materials like poly-L-lactic acid (PLLA), poly-caprolactone (PCL), collagen, silk etc. to mimic the lamellar structure and the mechanical properties of the

native disc as closely as possible[8,15,17-23]. Despite the fact that focusing on the two portions individually is very prevalent, IVD degeneration most often involves both areas of the disc and thus solutions containing both phases are necessary to be able to properly restore the function of the IVD[8,9]. Some designs of biphasic composites, with both AF and NP portions have been published and show that the development of biomimetic discs is feasible[30,32]. Lazebnik et al., (2011) fabricated a biphasic IVD composite, by electrospinning poly-caprolactone (PCL) fibers into an AF portion and using agarose solution for the NP portion[32]. They then seeded the scaffolds with porcine AF and NP cells and proved that in both analogues the cell attachment, proliferation and function was similar to the native disc[32]. On another research, Park et.al[24] created an *in vitro* model of IVD containing both of its analogues. On their scaffolds they seeded AF cells for the outside portion and chondrocytes encapsulated in a fibrin/hyaluronic acid (HA) NP hydrogel.

1.4 Tissue Engineering Limitations and Challenges

In spite of big, evolutionary steps made, therapy of IVD through tissue engineering still requires improvements, to be able to overcome a lot of challenges. Although several studies focus on eliminating issues with the scaffolding, such as morphology of the electrospun fibers, obliteration of a discreet boundary between the two phases and achieving appropriate mechanical properties of tension and compression moduli, there are far more issues, which mainly involve the cells source for IVD.

It has been proven that utilization of isolated disc cells and their re-insertion on a IVD retards the degeneration of the disc[25]. These AF and NP cells are capable of synthesizing the appropriate ECM required in the disc and already possess the necessary phenotype to function according to native tissue [25,27,28]. Sources for disc cell isolation can be the same

degenerative IVD, or neighboring tissue. However, discs are characterized by their sparse population of residing cells, which make up for only 1% of the total tissue volume[27-29]. Therefore, isolation of sufficient number of cells for the AF or NP regeneration is a challenge[27-29]. Furthermore, these cells do not have great proliferation ability, which renders it difficult to expand them for tissue engineering purposes[25, 27-29]. In addition to that, extraction and use of allogenic AF or NP grafts is proven to not be very effective, despite their lack of immunogenicity, making identification of new cell sources for IVD tissue engineering emerging and crucial[30].

1.5 Electrospinning of Scaffolds

Electrospinning is considered one of the most attractive techniques that exists for fabrication of scaffolds, due to the amount of benefits it offers[32-35]. Reason why there is such growing interest is that electrospinning allows for the fabrication of three dimensional, nanofibrous, and porous scaffolds that create an ideal environment for cell adhesion, proliferation and differentiation[36]. Moreover, it can utilize both synthetic and natural polymers, accordingly[32-36]. The process involves the fabrication of ultrafine fibers by electrically charging (with high voltage) a suspension droplet with a polymeric solution, which results in non-woven structures with high surface-to-volume ratio, a large ratio of which are in the form of interconnected pores[36-38]. As previously mentioned, porosity is important for scaffolds, to allow for transport of nutrients toward the cells and allow excretion of cell derived waste[39]. Ability to tune the morphologies and characteristics of the scaffolds arises from the different solution and processing parameters of the spinning; particularly polymer molecular weight, polymer concentration in the solution, applied

potential of the spinning apparatus and distance between needle and collector are a few of the parameters that can be modified depending on the necessities of the scaffold[37-39].

1.6 Rationale and Objective of Current Study

In lieu of the limitations that current IVD tissue engineering research is confronting, this research was focused only on the AF analogue of the discs and alternative cell sources that can be readily used to efficiently mimic the phenotypes and functions of the cells in native tissue. The approach that was used in this experiment was the co-culturing of porcine AF cells with marrow-isolated adult multilineage-inducible (MIAMI) cells, to study the effect of the disc cells in the differentiation and further functionality of the latter ones, towards a phenotype and behavior that mimics that of the native tissue.

MIAMI cells are a special population of marrow-stromal cells (MSCs) with the ability to proliferate extensively without undergoing senescence and loss of differentiation potential[40,44]. Generally, MSCs are a heterogeneous population, which involve uncommitted and/or lineage-committed cells that can differentiate into various lineages[40-51]. In the native bone marrow, MSCs contain subpopulations of primitive forms of the stem cells that have unique multipotent characteristics. The MIAMI cells, are non-transformed versions of the bone marrow MSCs that upon isolation from the tissue are treated under specific culture conditions that differ from the traditional ways of separating and handling of the MSCs[40]. These conditions involve specific ECM substrates, oxygen exposure percentage, growth factor and vitamin cocktails, cell density and co-culture of cells with other subpopulations, and are selected appropriately to mimic the niche microenvironments of the desired primitive stem cells, present in the native tissue[40]. One of the most crucial differences between treatment of the typical MSCs and the MIAMI cells, is that in the latter

one, the whole, unfractionated bone marrow is used, whereas in the traditional process the bone marrow is broken down[40]. In the case of the MIAMI cells, non-adherent and adherent populations are cultured together for a prolonged period of time, unlike the MSCs[40]. Lack of fractionation leads to the maintenance of some of the progenitor cells that play important roles in the niche signaling present in the native tissues, which can get lost during fractionation[40]. Moreover, the initial co-culturing with the non-adherent cells (that normally get removed in the traditional processes) is shown to allow for the survival of valuable, primitive progenitors, due to the presence of cytokines responsible for sustaining the viability and functionality of such cells[40]. MIAMI cells are also cultured in hypoxic conditions, in which the oxygen percent in the incubator is around 3% instead of the typical 21%. The special treating of the MIAMI cells allows for evident advantages over the MSCs. Namely, these cells have been proven to be capable of embryonic stem cell-like characteristics, involving increased expansion properties[40]. D'Ippolito et al., (2004) have proven that under conditions of 37ºC, 3% O_2, 5% CO_2, and 92% N_2, cells appear to have phenotypes similar to their stem-cell progenitors, with reduced cytoplasm, while expressing numerous, unique markers found in embryonic stem cells[40]. Particularly, MIAMI cells appear to be a homogenous population, expressing markers such as *Oct-4, hTeRT, Rex-1, SSEA*-4, and other markers from all three germ layers[40-42]. These properties of the MIAMI cells render them a good candidate for reparative medicine and an efficient cell source for tissue engineering.

As aforementioned, a big challenge in IVD tissue engineering, is identification of a cell source for seeding on scaffolds that is readily available. Numerous studies have focused on researching for alternative cells that can be used in place of AF and NP cells,

which are sparsely populated and hard to harvest. MSCs are more commonly used, due to the simplicity of their isolation and treating techniques, and the fact that they are multipotent and can yield different phenotypes[10,25,27,29]. Utilization of MSCs for IVD is widespread and has been proven that it is plausible to use these cells in co-cultures with small amounts of native disc cells to lead in phenotypes and behaviors close to the native tissue[10,25,27,29]. Particularly, Tsai et al., (2014) have indicated ratios of disc-to-MSCs that are evident to lead to differentiation and functionality of the MSC co-cultures similar to the native IVD one[10]. However, there are still a lot of limitations that exist with using MSCs; initially, mesenchymal stem cells are very heterogeneous, which creates issues with control of appropriate differentiation. Moreover, they still rely on big amounts of native AF to differentiate towards the required lineages, hence not eliminating the need for biopsy of the discs and the issue of scarcity of the cells[10,25-29]. Switching the MSCs for MIAMI cells, might create a more efficient cell source for the IVD regeneration, since MIAMI cells are closer to the MSC progenitor ones and have extensive viability and pluripotency capabilities. Moreover, the fact that MIAMI cells can be readily isolated from vertebral bodies[40-42] might allow for easier differentiation of these cells towards the native phenotypes, without requiring great amounts/ratios of AF cells. According to Tsai et al., (2014) 2:1 AF:MSCs was the ratio that allowed for the greatest differentiation of the MSCs into AF-like cells and the expression of proteins and markers close to the native tissue[10].

This research was focused on studying the behavior of porcine AF/MIAMI cells co-culture seeded on electrospun, polycaprolactone (PCL) scaffolds and their ability to differentiate towards specific lineages and function biomimetically to the native IVD tissue. The **hypothesis** was that seeding the co-cultures on the PCL scaffolds, in the

specific ratio of 2:1 AF/MIAMI would lead to effective differentiation of the latter ones towards native IVD lineages more efficiently than seeding MIAMI cells alone on the scaffolds. Appropriate differentiation of the MIAMI cells into AF, would mean that another cell source for IVD tissue engineering can become available, one that would be easier to obtain.

The objective of the study was approached by pursuing three **specific aims**. The *first one* was to develop an approach for fabrication of an annulus fibrosus construct, through electrospinning of nanofibrous scaffolds with random orientation. The *second aim* was to demonstrate that seeding the electrospun scaffolds with co-cultures of AF/MIAMI would lead to cell viability and functions similar to the native AF. AF/MIAMI co-cultures and controls were seeded on scaffolds for 3 weeks and samples for each group were assessed through imaging and biochemical assays. The *third aim* was to examine the possibility of AF cells alone to differentiate into other lineages and to predict possible variations and possibility of calcifications on the scaffolds. AF cells were thus treated with osteogenic media for three weeks and were assessed for osteogenic markers.

CHAPTER 2: MATERIALS AND METHODS

2.1 Electrospinning of AF Scaffolds

Annulus fibrosus scaffolds (d=10mm, h=1mm) were fabricated using different polymeric solutions and electrospinning with a custom apparatus, containing a syringe pump (New Era Pump Systems Inc., NY), a Bertan 230 high voltage power supply (Spelman, NY) and a glass slide covered with aluminum foil as a collector (**Figure 1.1A**). Polymeric solutions of 12%, 18% and 20% polycaprolactone (PCL) (Mw=80,000, Sigma) with dichloromethane (DCM) (Sigma-Aldrich, MO) or 1,1,1,3,3,3-Hexafluoroisopropyl alcohol (HFIP) (Chem-Impex Int'l Inc., IL) were prepared and were let to stir for ~30-45 minutes or until the polymer pellets were completely dissolved. After the samples were homogenous, they were loaded on 10ml syringes with 22G blunt-end needles. As shown in **Figure 1.1A**, the distance between the needle and the collector was kept at 10cm and the feeding flow rate for the electrospinning of the solution was set at 2ml/hr. A high voltage was applied between the needle and the grounded collector and was set to ~15kV. Randomly organized mats of non-woven fibers were collected on the aluminum slide. After the electrospinning process was completed, the mats were carefully removed from the collector, and excess solvent was evaporated. Using a punch, the scaffolds were cut into 10mm discs.

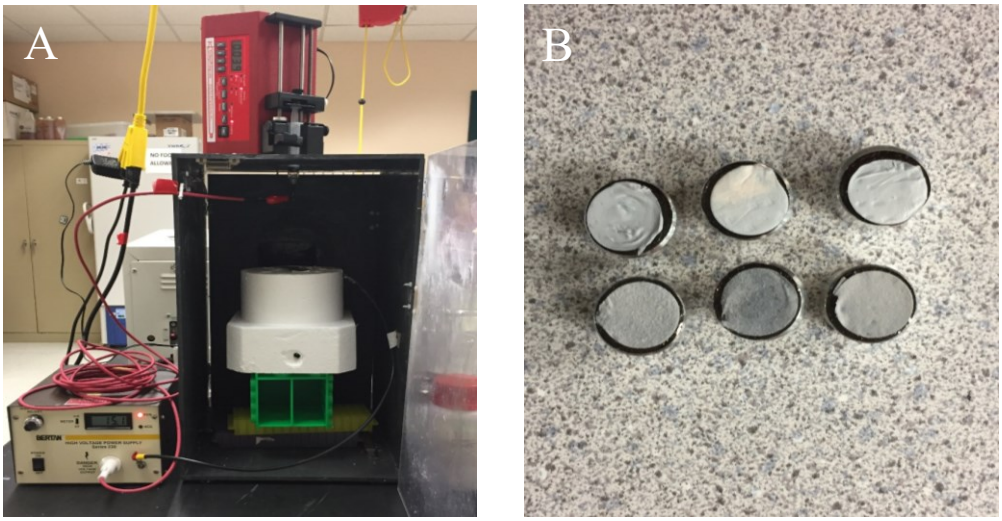

Figure 2.1 Electrospinning and imaging process. **A)** Electrospinning apparatus, containing the high voltage power supply (left) and the syringe pump (top, right). The red cable was connected to the needle and was supplying ~15kV, whereas the black cable was connected through an alligator clip onto the glass slide-collector and functioned as the ground. **B)** Thin layers corresponding to each of the scaffolds, before the SEM imaging. The top three are the PCL/DCM (15%, 18% and 20%), whereas the bottom three are for the PCL/HFIP (12%, 15% and 18%).

2.2 Scaffold Characterization

2.2.1 Cell Attachment and Biocompatibility Assessment

PCL electrospun scaffolds were tested for their ability to attach cells and to assess their ability to carry the future co-cultures, using GFP-MIAMI cells. 10mm diameter discs were excised from the electrospun mats with a punch and were sterilized for 1 hour under UV light. The scaffolds were then placed in a 48-well plate and expansion media comprising of 95% DMEM-low glucose (Thermo Fisher, MA), 3% fetal bovine serum (FBS) (HyClone Inc., UT), 1% HEPES (Thermo Fisher, MA),100 U/ml penicillin and 1000 U/ml streptomycin (Corning, NY), ascorbic acid (Sigma, MO) and a lipid solution was added to each well. To test the effect of media adsorption on the scaffolds and future cell

adherence, three scaffolds were incubated with the culture media for only 30 minutes, whereas three others were incubated with the media overnight.

Human MIAMI cells (fifth passage), tagged with GFP were trypsinized upon reaching 80% confluence. Particularly, the culture media was aspired and 10ml of trypsin-EDTA (Thermo Fisher, MO) were added to allow the cells to detach from the fibronectin covered T-175 flasks. Once the cells were detached, the trypsin reaction was quenched with 5ml expansion media (95% DMEM-low glucose, 3% FBS, 1% HEPES, 1% antibiotics, ascorbic acid and lipid solution). The cells were then centrifuged to remove the supernatant and 10ml of new media was added. Cells were seeded on the scaffolds at a density of 150,000 cells/scaffold, dropwise. Briefly, the culture media was aspired from the 48-well plate and 20μl of the cell solution was added dropwise on the center of the scaffolds using a pipette. Cells and scaffolds were incubated in low-oxygen conditions for 30 minutes to enable attachment. Afterwards, 300μl of fresh expansion media were added on each sample and the plates were incubated for 72hr. Cell adherence on the scaffolds was observed under a confocal microscope. The constructs were imaged to assess location of attachment of the cells and to establish whether or not the PCL scaffolds were capable to function as carriers for the future co-cultures.

The biocompatibility of the scaffolds was determined by viewing the seeded scaffolds under the microscope, as well as by detaching the cells from the scaffolds and performing a live/dead assay. Particularly, the PCL discs were removed from the wells containing the expansion media and were placed in new, sterile ones. 100μl of trypsin were added onto the scaffolds and the plates were incubated for 3-4min to allow detachment of cells. For the wells containing the media were the scaffolds used to be, 300μl of media were removed

and stored in a conical tube as saved media. 300μl of trypsin were added on the wells and they were incubated for 2min to allow detachment of any cells possibly attached on the well walls. Trypsin action was quenched by adding 100μl of fresh culture media on the scaffolds and the 300μl of the saved media into the wells. Mixtures from both the scaffolds and the wells were pipetted into different conical vials and were centrifuged at 400G for 5min. The supernatant was then removed and 1ml fresh media was added in all tubes. The cells were stained with trypan blue (Corning, NY) and were counted. A comparison between live and dead cells present on the scaffolds and in the wells was performed.

2.2.2 Scanning Electron Microscopy Imaging

Acellular scaffolds for each of the aforementioned concentrations and polymeric solutions were imaged using JSM-6010 Plus (JEOL, Japan) scanning electron microscope, and information on the fiber morphologies and diameters was obtained. Particularly, thin layer-samples for each of the scaffolds were obtained and placed on supporting cylinders (**Figure 1B**). Before imaging, the samples were spur-coated with gold for ~15sec. Following that, they were placed in the SEM and were imaged in varying magnifications x500-x2,000.

To determine the diameters of the fibers for each of the different scaffold compositions, Image J (National Institute of Health, MD)[52] was utilized. The software was calibrated using the scale bar present at each SEM image. To follow a specific pattern in the selection of fibers, the average fiber diameter was determined after measuring the diameter of 10 randomly selected fibers from each four corners of the obtained SEM

images. A total for 40 calculations per sample were obtained. Finally, observation of the distribution of the fiber diameter calculations was determined and plotted.

2.3 Cell Isolation and Culturing

2.3.1 Cell Extraction

Annulus fibrosus cells were obtained from the lumbar intervertebral discs of a female, 3-year old pig. The protocol used for the isolation and culturing of the disc cells was that indicated by Tsai et al., (2014)[10]. Particularly, the AF portion of three discs was separated from the NP core and was diced using a scalpel. Collagenase A digestion followed up, where 0.054g of collagenase A (Thermo Fisher, MA) were dissolved in a 54ml IVD culture media comprised of 45% low-glucose DMEM (Thermo Fisher, MA), 45% F12 (Thermo Fisher, MA) 10% FBS and antibiotics/antimycotics (Corning, NY). The collagenase A digestion was carried out on an orbital shaker, in an incubator (21% O_2, 5% CO_2) at 37^{o}C for 16 hours. After the digestion was completed, the cells were filtrated twice, through a 100μm and 40μm cell strainer and were centrifuged for 5min at 400G. Resulting cell pellets were split in half and re-suspended in fresh IVD culture media (89% low-glucose DMEM, 10% FBS and 1%antibiotics). The cells were plated and cultured in T-75 cell culture flasks in 5% CO_2 incubator and their media was changed every two days. Cells were passaged upon reaching 80% confluence. Cells of the 2nd passage were used.

Secondary MIAMI cells were obtained by the GRECC and Research Service (Bruce W. Carter Miami VA Healthcare Center, FL). The cells had been previously isolated and cultured following the protocol described by D'Ippolito et.al [40,50,64]. Namely, porcine bone marrow cells were isolated from cadaveric thoracolumbar vertebral bodies. Whole bone marrow, which did not undergo fragmentation, was seeded at a density of ~10^5

cells/cm^2 on fibronectin coated plates that contained low-glucose DMEM which contained 5% FBS, 100 U/ml penicillin and 1000 U/ml streptomycin. Co-cultures of adherent and non-adherent cells were maintained in the incubator under 3% O_2, 5% CO_2, and 92% N_2 for approximately 14 days. During that time, the non-adherent cells were removed. Afterwards, single-cell derived colonies of adhered cells were obtained by plating the remaining cells at a 0.1-0.2 cell/cm^2 density. From those colonies, some (50-100 cells) were selected and were carefully removed by rinsing with trypsin-EDTA (Thermo Fisher, MA). The cells were then plated at a 1.3x10^3 cells/cm^2 on fibronectin-coated dishes with an expansion medium containing 92% DMEM-low glucose, 5% FBS and penicillin and streptomycin at 3%. The incubation conditions of the MIAMI cells were 3%O_2, 5% CO_2, 92% N_2, and the cells were expanded at low density of ≥30% confluence.

2.3.2 AF/MIAMI Cells Co-Culture and Cell Seeding

Upon reaching confluence, porcine AF and MIAMI cells were trypsinized and mixed in conical tubes at ratio of 2:1 AF/MIAMI. Two control groups were created, a positive one, containing only AF cells, and a negative one, with only MIAMI cells. Controls and co-cultures of cells were seeded on the electrospun scaffolds, at a density of 120,000 cells/scaffold. The seeded scaffolds were then immersed in IVD culture medium (89% DMEM-low glucose, 10% FBS, and 1% antibiotics pen-strep) and placed in the incubator for 3 weeks. *In vitro* tests were performed at 0, 2 and 3 weeks, and the culture media was changed every two days. A total of 30 scaffolds were prepared for the two controls (only AF, only MIAMI) and the co-culture (2:1 AF/MIAMI). Simultaneously to the experiment, the three groups of cells (AF-, MIAMI-only, and co-cultures) were seeded

without substrate on 12-well plates at a density of 120,000 cells/well. Samples were obtained at week 0, 2, and 3.

2.4 AF Differentiation

In a study performed by Liu et.al (2014), it was shown that there are stem cells derived from AF that can differentiate into osteocytes, chondrocytes and adipocytes[53]. In this study, we determined the ability of AF to proceed through direct osteogenesis, as a way to study possibility of AF differentiation and calcification in our AF/MIAMI co-cultures. The previous protocol for osteogenesis in AF-derived stem cells, which was described by Liu et. al (2014)[53] was followed. Briefly, annulus fibrosus cells of second passage were plated in 6-well plates at a density of 50,000 cells/well. Cells were cultured in a basic culture media, comprising of low glucose-DMEM and 1% penicillin and streptomycin, until 80% confluence. The media was then aspired and the cells were cultured in an osteogenic media (basic culture media containing 0.1μM dexamethasone, 0.2mM ascorbic-2-phosphate and 10mM glycerol-2-phosphate) for three weeks. To assess differentiation of the AF cells towards osteogenic lineages, histology staining and RT-PCR were performed.

2.5 Biochemical Assays

2.5.1 Total RNA Isolation and Reverse Transcription PCR

Total RNA was isolated from the scaffolds using TRIzol reagent (Invitrogen, CA) and following the manufacturer's protocol. Particularly, each sample was placed in an Eppendorf tube, and 1ml of the TRIzol reagent was added. The samples were let to incubate

for 45min at 4ºC, at which time the scaffolds were dissolved in the reagent. Scaffolds that were not dissolved fully were removed with a sterile, RNase/DNase-free pipette tip. Afterwards, 0.2ml of chloroform (Mallinckrodt Chemicals Int'l, UK) were added and each sample was briefly vortexed and incubated for 5min at room temperature. Upon incubation, the samples were centrifuged at 12,000G for 15min, to allow for separation of the layers into an aqueous (containing the RNA), an intermediate (containing proteins) and a bottom, organic one (containing DNA and proteins). Using a micropipette, the aqueous phase located in the top of the tube was collected and transferred into a new Eppendorf tube. Since the RNA amounts expected were low, 5g of RNase-free glycogen (Qiagen, Germany) were added to the isolated aqueous phase to allow for better visualization after precipitation. To precipitate the RNA, 0.5ml of 2-propanol (Sigma-Aldrich, MO) were added in the tubes, and the samples were let to incubate at room temperature for 10min. Following the incubation, samples were centrifuged for 10min at 12,000G at 4ºC and the supernatant was removed. The RNA was then washed by re-suspending the RNA pellet in 1ml 75% ethanol (Sigma-Aldrich, MO) and vortexing briefly. The ethanol supernatant was then removed by centrifuging at 7,500G for 5min. The RNA pellet was set to air dry for 10min, for complete removal of any ethanol residues. The pellets were then resuspended in 40μl of RNase-free water and were incubated on a heat block (55ºC) for 10-15min, to allow for complete dissolution of the RNA in the water (no visible pellet).

For the RNA isolation of the cells cultured without substrate, on the 24-well plates, the TRIzol reagent was utilized, however, following the manufacturer's protocol some steps varied from the ones previously described in the scaffold protocol. Particularly, culture media from the wells was carefully removed. The cells were not washed with PBS;

instead, 400µl of TRIzol reagent were placed straight onto the well and the solution was mixed/homogenized by pipetting up/down for five times. Samples were let to incubate in TRIzol for 5min at room temperature. By that that time, 80µl of chloroform were added in each tube and the samples were vortexed briefly and incubated for 5min at room temperature. To separate each sample into the three distinct layers or RNA, DNA and proteins, each tube was centrifuged, as previously mentioned, at 12,000G, at 4ºC for 15min. The aqueous layer containing the desired RNA was isolated and placed in a new, clean tube. To maintain the protocol consistent, 5g of RNase free glycogen were added to each tube, to better visualize the pellet. The samples were washed with 200 µl of 2-propanol by incubating for 10min at room temperature and then centrifuging at 12,000G for 10min at 4ºC. Upon removal of the supernatant, 400 µl of ice-cold, 75% ethanol were added, and the samples were centrifuged for 5min at 7,500G. Ethanol was removed carefully, so as not to aspire the RNA pellet, the samples were air-dried for 10min, and then 40µl of RNA-grade water were added to each tube.

Total RNA was quantified using a Nanodrop200c spectrophotometer (Thermo Scientific, MA), set to detect the absorbance of nucleic acids. A drop (1µl) of each of the samples was used to create a plot of the absorbance versus the wavelength (nm) and determine the concentration (ng/µl) of nucleic acids present, as well as determine the purity of the sample, through 260/280 and 260/230 observations. RNase-free water, used in the previous step was used to blank the machine after every trial. Samples frozen in -80º were thawed at the end of the 3-week period for downstream PCR.

For the following reverse transcription, set amounts of RNA were used. Particularly, upon RNA quantification, samples were either diluted or concentrated with

RNase-free water, to reach a final mass of 1μg of RNA in 10μl of water. To concentrate samples with small amounts of RNA, an ethanol precipitation protocol was performed. Particularly, 0.1 volume of 3mM sodium acetate (pH 5.2), 3 volumes of ice-cold ethanol and 7μl of RNase-free glycogen were added in each tube. The samples were briefly vortexed and then incubated at -20ºC overnight to allow for maximum RNA precipitation. Samples were then centrifuged at 13,000G for 30min at 4ºC and the supernatant was removed. To wash the pellet, 0.5ml of 75% ice-cold ethanol were added in each sample and the tubes were centrifuged at 13,000G for 10min (4ºC). The ethanol was removed, the tubes were centrifuged at max speed for 10s to dry, and these steps were repeated one more time. Upon completion, samples were let to air-dry for 15min and were then resuspended in the appropriate amount of water, to reach a final concentration of 100ng/1μl.

After the samples were eluted, the RNA was reverse transcribed into complementary DNA (cDNA) using a High Capacity cDNA Reverse Transcription Kit (Thermo Fisher, MA). Briefly, RNA samples were thawed on ice. A transcription master mix was prepared by mixing 2μl of RT buffer, 0.8μl of dNTP mix (100mM), 2μl of random primers, 1μl of MultiScribe™ reverse transcriptase, 1μl of RNase inhibitor, and 3.2μl RNase-free water per sample tube. A total of 10μl of the master mix was added in each PCR tube and was mixed properly by pipetting up and down. For this step, 1μg RNA was used for all samples. Hence, samples were either diluted or concentrated in 10μl of RNase-free water and were then placed in the PCR tubes. The tubes were then sealed and briefly centrifuged to spin down the contents and to remove any air bubbles present. The samples were loaded in a Stratgene Mx3005P cycler (Agilent Technologies Inc., CA) that was programmed into optimal conditions **(Table 2.1)**. The reaction volume was set to 20μl.

Reverse-transcribed samples were placed at 4ºC (short-term) or -20ºC (long-term) before performing PCR.

Table 2.1 Thermal cycler programmed conditions

	Step 1	**Step 2**	**Step 3**	**Step 4**
Temperature	*25 ◦C*	*37 ◦C*	*85 ◦C*	*4 ◦C*
Time	*10min*	*120min*	*5min*	∞

Before amplification of the cDNA, samples were purified using a PCR purification kit (Qiagen, Germany) and following manufacturer's protocol. Particularly, buffer PB was added in a ratio of 5:1 volumes (buffer:PCR samples). To bind the DNA, samples were loaded on a QIAquick column and were centrifuged at 17,900G for 30-60s. The flow-through was then discarded and 0.75ml buffer PE were added to the column to wash it. The column was centrifuged one more time at 17,900G for 30-60s. After the supernatant was discarded the column was centrifuged at 17,900G for an additional minute before being placed into a new 1.5ml microcentrifuge tube. To elute the DNA, 50µl of RNase-free water were added to the center of the membrane and were centrifuged at 17,900G for 1min.

For the PCR, the Brilliant II SYBR Green qPCR master mix (Agilent Technologies Inc., CA) kit was used. Particularly, a 15µl/tube mix was prepared comprising of 12.5µl SYBR master mix, 0.375µl ROX reference dye (previously diluted 1:500), 0.125µl RNase-free water and 2µl of 4mM primer solution (containing primers with forward and reverse sequences). **Table 2.2** shows the primers and their sequences used in this study. After the mixture was ready, the 15µl of master mix were combined with 10µl of purified cDNA (10x diluted in Nuclease-free water). The samples were briefly centrifuged to remove any gas bubbles formed and were loaded on the Stratgene Mx3005P cycler. The conditions for

the PCR that were programmed on the cycler are given in **Table 2.3**. Data was collected automatically with the Mx3005P software (Agilent Technologies Technologies Inc, CA)

Table 2.2 RT-PCR Porcine Primers

Gene		Sequence
Acan	F	5'-GTTCAAGCCAATCCACTGGT-3'
	R	5'-CAGTCACACCTGAGCAGCAT-3'
Alk-P	F	5'-ATGAGCTCAACCGGAACAA-3'
	R	5'-GTGCCCATGGTCAATCCT-3'
Col I	F	5'-CCAAGAGGAGGGCCAAGAAGAAGG-3'
	R	5'-GGGGCAGACGGGGCAGCACTC-3'
Col II	F	5'-CAGGTGCTGCAAGTCTTCCT-3'
	R	5'-GAAGTCCCTGGAAGCCA-3'
ELF-1a	F	5'-CCACCACTACTGGCCATCTG-3'
	R	5'-ACGCTCACGTTCAGCCTTTA-3'
IBSP	F	5'-CGACCAAGAGAGTGTCAC-3'
	R	5'-GCCCATTTCTTGTAGAAGC-3'
Nanog	F	5'-ATCCAGCTTGTCCCCAAAG-3'
	R	5'-ATTTCATTCGCTGGTTCTGG-3'
Oct-4	F	5'-AGGTGTTCAGCCAAACGACC-3'
	R	5'-TGATCGTTTGCCCTTCTGGC-3'
Osteocalcin	F	5'-TCAACCCCGACTGCGACGAG-3'
	R	5'-TTGGAGCAGCTGGGATGATGG-3'
Osterix	F	5'-CTCATTCCCTGGGCTCAC-3'
	R	5'-TGGGCAGACAGTCAGAAGAG-3'

Aggrecan (Acan), Alkaline phosphatase (Alk-P), Collagen I and II (Col I and II), Elongation factor (ELF-1a), Integrin binding bone sialoprotein (IBSP), Nanog homeobox (Nanog), Octamer-binding transcription factor 4 (Oct-4),Osteocalcin and Osterix. F: forward, R: reverse.

after the annealing phase (56◦C) and at the end, during the melting phase (after the 55◦C step). Amplification plots were plotted (fluorescence vs. cycles). The expression of various genes in the samples was determined by utilization of the $2^{-\Delta\Delta Ct}$ method. Samples were run in duplicates for each of the genes studied. Positive reactions of the samples with the primers were identified through fluorescence, in which case, the cycle threshold value (Ct) was obtained and used in further analysis. The threshold value was automatically calculated and set by the Mx3005P software, such to differentiate positive results from background fluorescent signal.

Table 2.3 PCR Thermal cycler conditions

Cycle(s)	*Time*	*Temperature*
1	10min	95◦C
40	30sec	95◦C
	1min	56◦C
	1min	72◦C
1	1min	95◦C
	30sec	55◦C
	30sec	95◦C

Genes were quantified upon obtaining the Ct values of each sample and their replicates, using the $2^{-\Delta\Delta Ct}$ technique. Particularly, an Excel spreadsheet was prepared for each gene and sample (AF and MIAMI controls, co-cultures for the different weeks). *ELF-1a* was the only housekeeping gene that was used to normalize the data. Before initiating the analysis of the data, the Ct values obtained from the replicates of each sample for each gene were averaged. Replicates with Ct values variating more than 1 unit were discarded, due to the fact that differences in the units of Ct mean two-fold differences in the amount/expression of the gene.

2.5.2 Histology

AF cells treated with osteogenic media on culture tissue plates were fixed and stained for alkaline phosphatase after incubation for three weeks, to determine their ability to directly differentiate towards osteogenic lineage and possibility of calcifications forming on the scaffolds. Initially, the media was removed from the samples and the wells of the 6-well plate were rinsed with warm DPBS to remove any traces of remaining media. 2ml of 70% ethanol were then added on each sample and the plates were incubated for 30min at −4ºC to fix the samples. In the last step of the fixing, ethanol was removed and replaced

with distilled water and the samples were stored at -4ºC until staining. For the histochemical analysis of alkaline phosphatase activity, 8mg of naphtol AS-TR phosphate disodium salt (Sigma, MO) were dissolved in 0.3ml N, N-dimethylformamide (Sigma, MO). Simultaneously, 24mg Fast Blue (Sigma, MO) were dissolved in 30ml of 0.1M Tris buffer (pH 9.6) (Corning, NY). The two solutions were mixed, and the solution was adjusted to pH 9.0. Upon an addition of 10mg $MgCl_2$, the solution was filtered and used immediately. Particularly, 2ml of the alkaline phosphatase stain were added in each well, and the samples were incubated at 37ºC for 30min. Before imaging with the microscope, the stain solution was aspired with a pipette and the samples were rinsed thrice with DI water. Imaging of the plated containing the stained cells was performed using a confocal microscope.

2.6 Statistical Analysis

The results that concluded are presented in the form of mean ± standard deviation. Normality of the data obtained was determined by utilizing the Shapiro-Wilk test. For the analysis of the fiber diameter data, a one-way analysis of variance (ANOVA) test was performed. Differences between the data were considered significant for $p<0.05$ and those data were further processed using a Tukey multiple comparison test.

CHAPTER 3: RESULTS

3.1 Scaffold Characterization

After scaffolds were fabricated through electrospinning, images of their fibers were obtained using scanning electron microscopy (SEM). Independently of the solvent, all scaffolds appeared to possess random orientation in their fibers (**Figure 3.1**). However, the fiber diameters and their uniformity varied between polymeric solutions containing DCM and HFIP. Solutions containing DCM resulted in fibers with great deviations in their diameters ranging from a couple to several tens of microns (**Figure 3.1 A-C**). As for the overall alignment of the scaffolds, PCL/DCM scaffolds were randomly organized, with fibers forming curls and beads (**Figure 3.1 A-C)**.

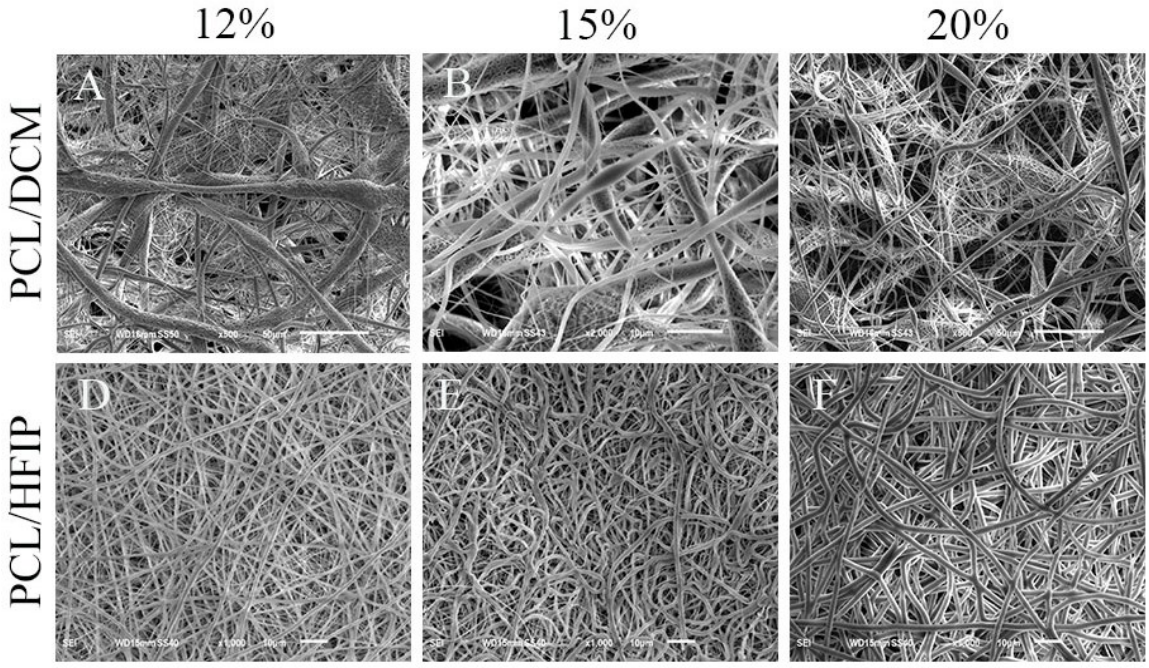

Figure 3.1 SEM images of the acellular scaffolds. Image of the 12% PCL/DCM scaffold at a x500 magnification **(A)**, 15% PCL/DCM scaffold at x2,000 magnification **(B)**, 20% PCL/DCM scaffold at a x500magnification **(C)**, 12% PCL/HFIP scaffold **(D),** 15% PCL/HFIP scaffold **(E),** 20% PCL/HFIP scaffold **(F)** at x1,000 magnifications.

Using ImageJ, the mean fiber diameter for each of the samples was calculated. Particularly, for the 12%, 15% and 20% PCL/DCM scaffolds the average fiber diameters were found to be 2.30±2.46, 1.21±1.18 and 2.73±1.86μm respectively. For the PCL/HFIP scaffolds the fiber diameters were calculated to be 0.88±0.27, 0.94±0.35, and 2.07±0.18μm for concentrations of 12%, 15% and 20% respectively (**Figure 3.2**). Using the Shapiro-Wilk test it was determined that all scaffolds comprising of PCL/HFIP possessed diameters following a normal distribution, as shown in **Figure 3.3**. The fiber diameters of the PCL/DCM scaffolds were found to not be normally distributed and therefore is not shown here.

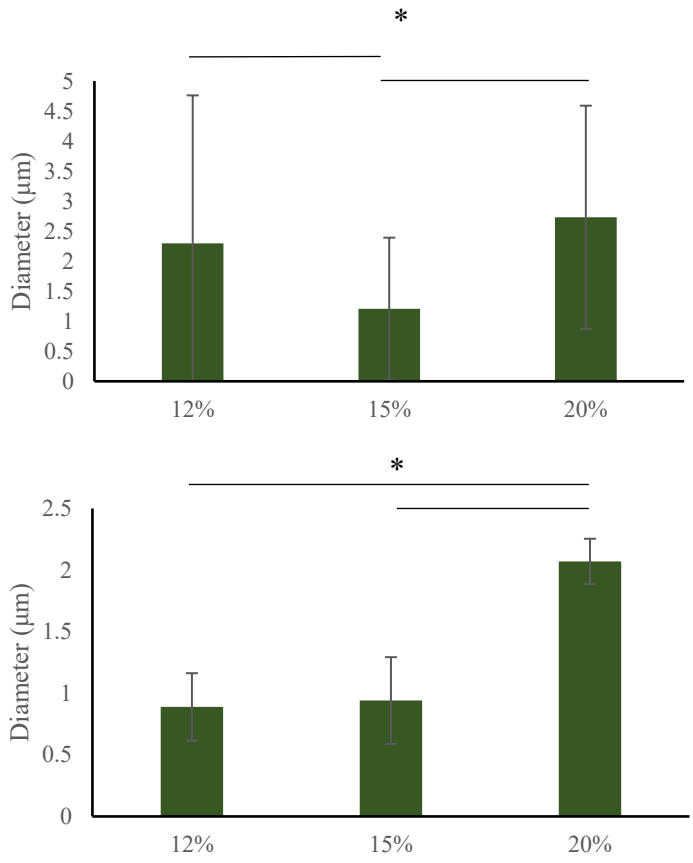

Figure 3.2 Fiber diameter of scaffolds. The average fiber diameter of scaffolds was determined using ImageJ. **A)** Mean fiber diameters (μm) for PCL/DCM scaffolds at concentrations of 12%, 15%, and 20%. **B)** Mean fiber diameters (μm) for PCL/HFIP scaffolds at concentrations of 12%, 15%, and 20%. (*) demonstrates a significant difference ($p<0.05$) between groups.

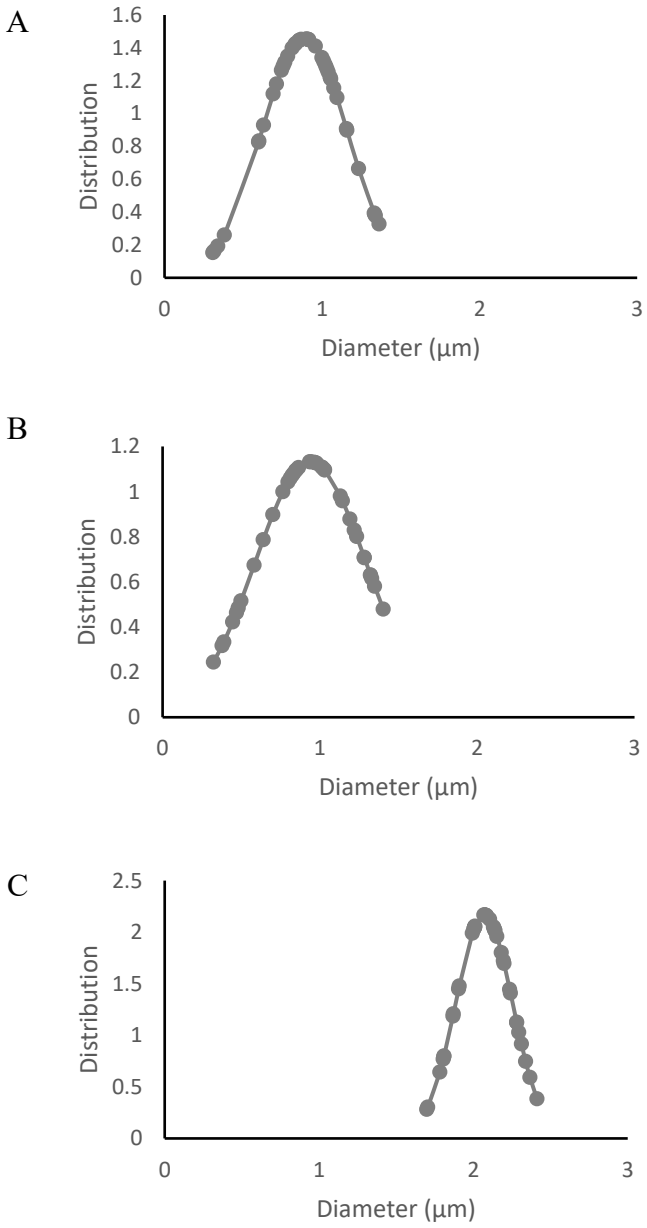

Figure 3.3 Fiber distribution for PCL/HFIP scaffolds. Graphs of the distribution of the 40 measured diameters per scaffold for **A)** 12% PCL/HFIP, **B)** 15% PCL/HFIP, and **C)** 20% PCL/HFIP. Normality of each of the samples was determined with Shapiro-Wilk test ($p<0.05$). Scaffolds containing PCL/DCM were not normal and therefore their distributions are not depicted.

Scaffold ability to attach cells and sustain their viability was determined by fluorescent confocal microscopy on PCL constructs seeded with green-fluorescent (GFP) MIAMI cells. To prepare the constructs for cell culture, they were incubated for a period of either 30min or overnight (16hr) in MIAMI expansion media. Cells appeared to attach well on the scaffolds, for both cases (data not shown) and initially occupied the scaffolds circumferentially. Moreover, scaffolds incubated overnight had the largest cell adherence. Tracing of GFP staining allowed the identification of the location of the attached cells on the scaffolds. As shown in **Figure 3.4**, cells were found mainly on the outer surfaces, but also deeper within the scaffolds. The cells were aligned around the edges of the constructs and were following the disc shapes (**Figure 3.4B)**. Cells did not appear to "slip" out of the scaffold, as there were no cells on the plate underneath the scaffolds (**Figure 3.4B)**. Cells cultured on the scaffolds possessed different phenotypes than cells cultured on plates (**Figure 3.4A, 3.4C**), which was concluded to be due to cells expanding in the orientation and between the fibers of the substrate.

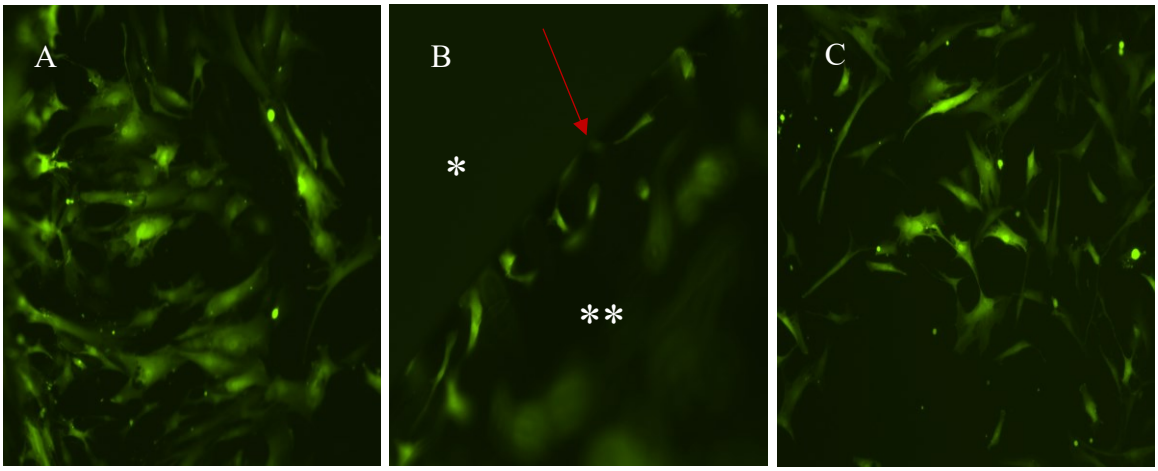

Figure 3.4 GFP-MIAMI cell adherence on scaffolds. GFP-MIAMI cells were seeded on the PCL scaffolds for 72hr to check for cell adherence and viability. Expression of GFP on the scaffolds demonstrated that cells were present both on surface and within the construct, suggesting them as good carriers of cells. **A)** Cells cultured on plain plates. **B)** Cells were present in abundance on the scaffolds and were aligned in the edges, compared to the plate that did not show signs of cells. The red arrow indicates the boundary between scaffold and plate. (*) plate and (**) scaffold surface. **C)** Cells on the center of the PCL scaffold.

Additional studies that were performed were to show that the adherence of the cells on the scaffolds was reversible; MIAMI cells attached on scaffolds for 72hr were detached using Trypsin-EDTA. As previously observed through microscopy, no cells were present on the plates underneath the scaffolds and hence trypsinization of those did not yield any cells. Some cells seeded on the scaffolds were able to get detached, however, that required long incubation times and yielded very small amounts of cells compared to the initial culturing density. This suggested that cells attach well on the scaffolds and cannot be removed easily. Hence for the *in vitro* PCR studies, scaffolds were dissolved to obtain the maximum amounts of cells.

3.2 AF Osteogenesis

Porcine AF were cultured in either plain IVD culture media or osteogenic media. Images of the cultured cells were obtained under the microscope at week 1, 2 and 3, from random locations on the culture plates. After culturing for 3 weeks, there were no distinct phenotype variations between the control and the osteogenesis groups (**Figure 3.5**). The cells were very confluent and were round in appearance.

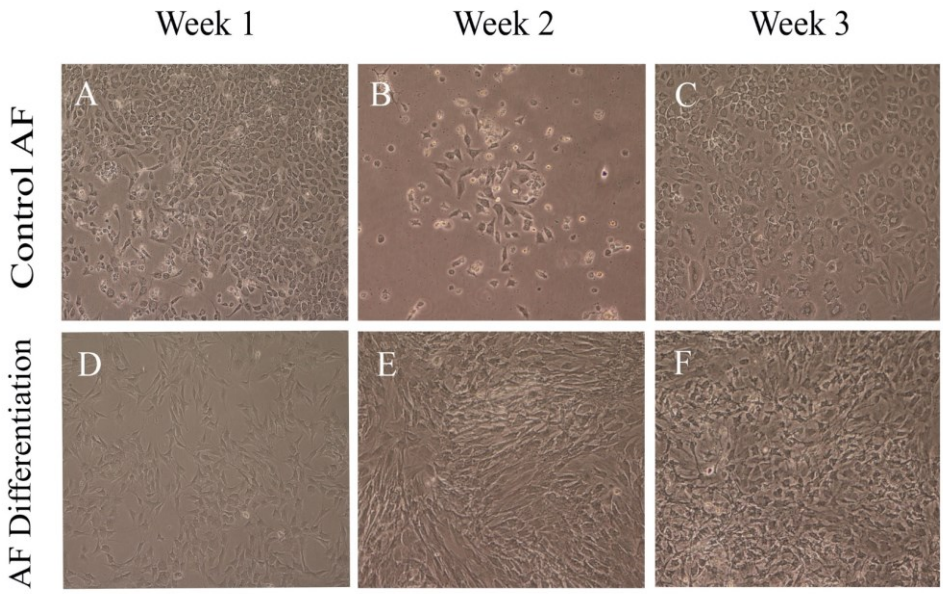

Figure 3.5 Phenotypic differences between control and differentiated AF cells. Annulus fibrosus cells were cultured in either basic IVD culture media (**A-C**) or osteogenic media (**D-F**), for three weeks. Images of the cultures were captured at weeks 1, 2 and 3. The cells did not show distinct phenotypic differences.

To better distinguish differences between the cells and to determine ability of the AF cells to differentiate under particular conditions, staining with alkaline phosphatase (*Alk-P*) was performed. As shown in **Figure 3.6**, AF cells were stained positive for *Alk-P*, which confirmed osteogenesis in the AF population.

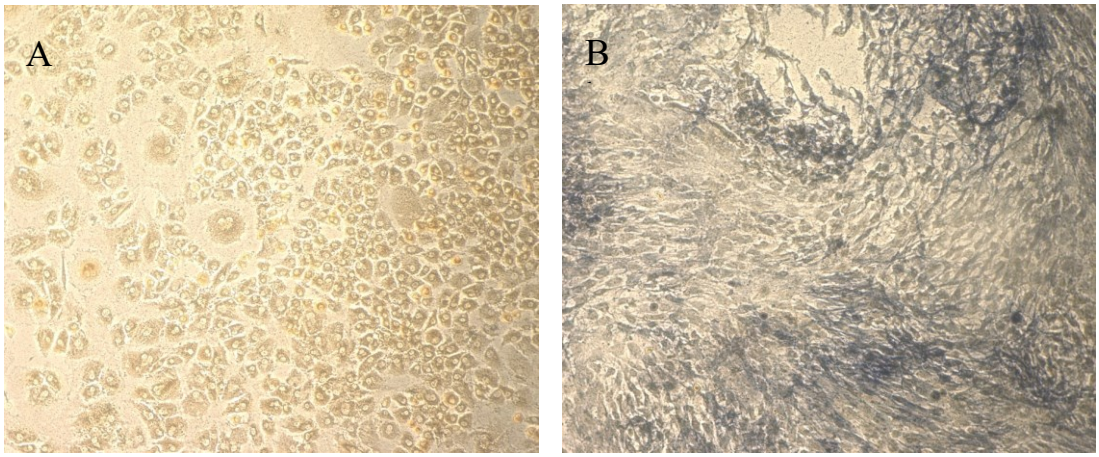

Figure 3.6 Alkaline Phosphatase staining of treated AF cells. AF cells treated with the osteogenic media for a three-week period were stained for alkaline phosphatase, an osteogenic marker. **A)** Control group of AF cells grown for three weeks in basic IVD culture media (no additives). No presence of the characteristic blue color indicates no presence of the marker. **B)** AF cells treated with osteogenic media for three weeks retained their normal phenotype, however, they were positive for the osteogenic marker (in small amounts).

3.3 Reverse Transcription PCR and RNA Expression

Total RNA expression was determined for the following sample groups: cells (AF-only, 2:1 AF/MIAMI, and MIAMI-only) seeded on scaffolds obtained at weeks 0, 2 and 3, and cells seeded without a substrate (on 24-well plates) obtained at weeks 0, 2 and 3. Additionally, AF RNA samples that either underwent osteogenesis or not (control), were obtained at weeks 0 and 3. Expression of the genes mentioned in **Table 2.1** was tested. For differentiation towards the AF lineage, *Col 1, Acan,* and *Col 2* were used as markers, while MIAMI markers *Oct-4* and *Nanog* were used to test for any undifferentiated populations in the samples. For the osteogenesis studies, *IBSN, Alk-P, Osteocalcin* and *Osterix* were used as positive markers.

Figure 3.7 shows the amplification curves for samples obtained at weeks 0, 2 and 3. AF-only and co-cultures seeded on scaffolds appeared to be positive for expression

targets for *Col 1* and *Acan* (**Figure 3.8A, 3.8B, 3.8C**). These samples showed expression of the housekeeping gene, which allowed for normalization of the data. Further analysis of the week 0 and 3 scaffolded samples, showed that collagen expression was increased in the AF and co-cultures and that expression of *Acan* was positive but very small compared to that of *Col 1* (**Figure 3.7**).

Despite the presence of distinct peaks in the scaffolded samples at weeks 0, 2 and 3, the samples containing the MIAMI control (MIAMI-only), as well as cell groups seeded on culture plates appeared to have great variations, with random Ct values between replicates and/or absence of amplification plots. For samples that contained duplicates with Ct value differences >1, no further analysis was performed. Samples that contained duplicates, for which one of the two samples did not show amplification curve were not considered for further analysis. Finally, the expression of the remaining markers yielded negative results and is hence not shown here.

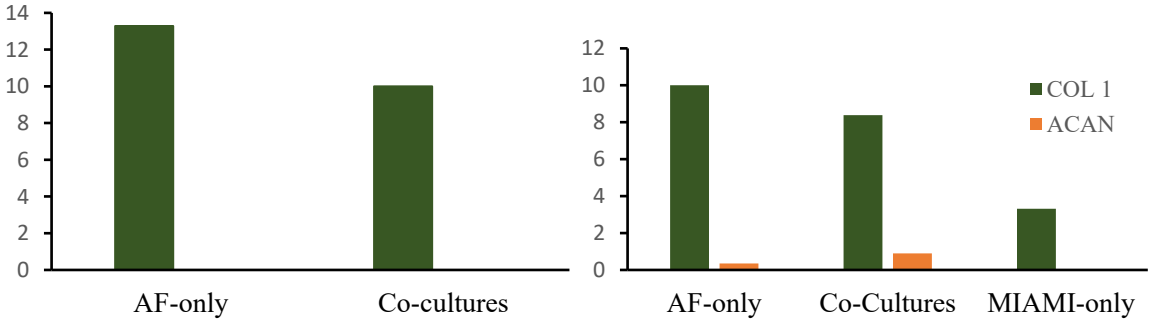

Figure 3.7 Gene expression in AF studies. Cells seeded on scaffolds expressed *Collagen type I* (COL 1) and *Aggrecan* (ACAN), determined by the analysis of the Ct values obtained from RT-PCR. The AF-only and co-cultures appeared to have increased *Collagen I* and *Aggrecan* expression compared to the MIAMI-only control.

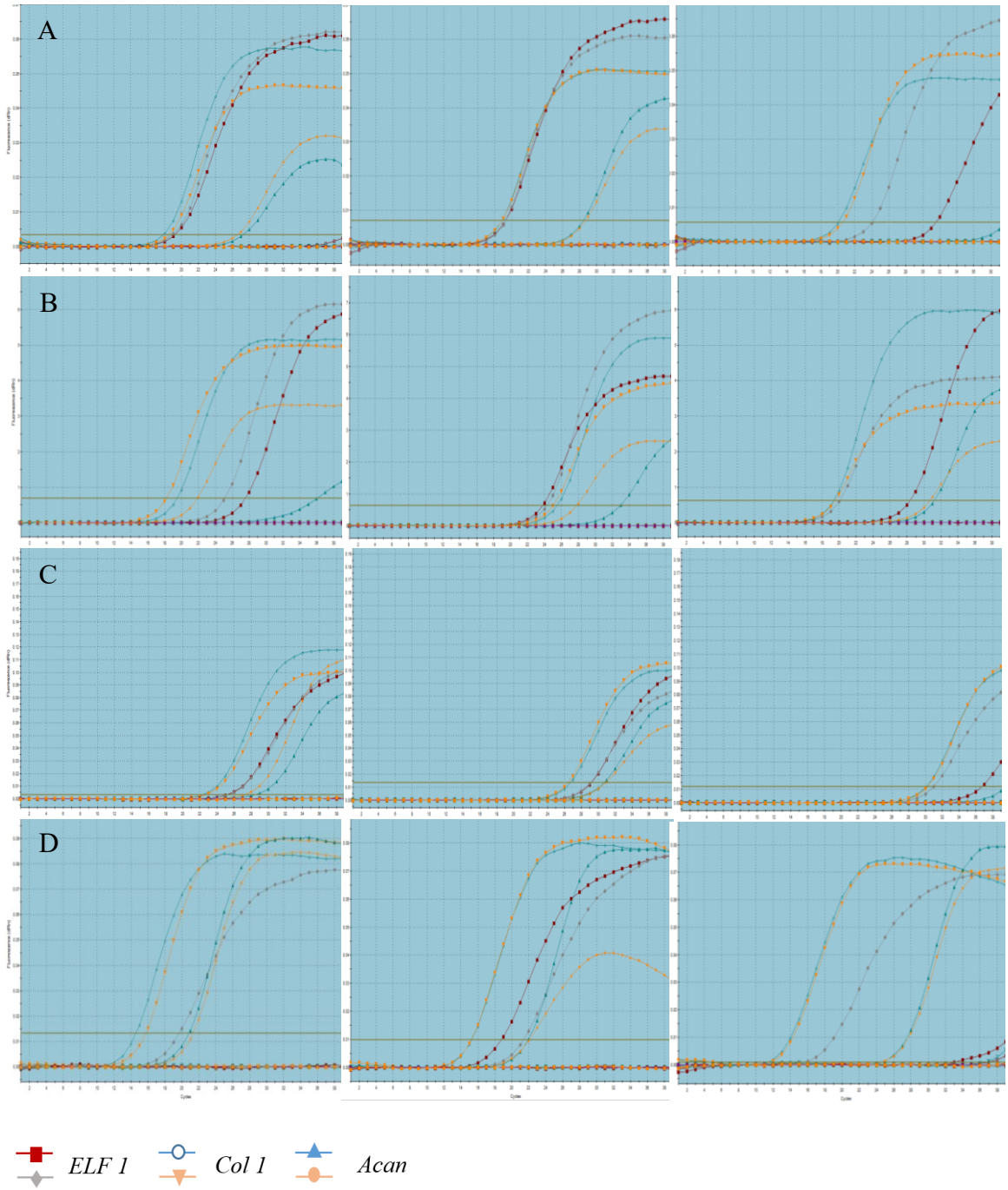

Figure 3.8 PCR amplification plots for AF lineage studies. Fluorescence (dRn) on the y-axis versus amplification cycles on the x-axis for AF-only, co-cultures and MIAMI-only samples for week 0 **(A)**, week 2 on scaffolds **(B)**, week 3 on scaffolds **(C)**, and week 3 without scaffolds **(D)**. The threshold value for each sample was automatically calculated, using the Mx3005P software (Agilent Technologies Inc., CA). Replicate samples with Ct value differences less than 1 were considered acceptable.

Reverse transcription PCR in weeks 0 and 3 samples for the control AF (under normal culturing conditions) and osteogenesis AF (in osteogenic media) was performed, as mentioned previously. Samples of week 0 did not give any positive markers for the osteogenic primers tested and are hence not shown here. After three weeks of culturing, samples in osteogenic media were tested positive for the expression of several markers (**Figure 3.9**); *Alk-P, Osteocalcin* and *Osterix* were present in the osteogenic AF, whereas the control group only appeared to have small expression of *Osteocalcin.*

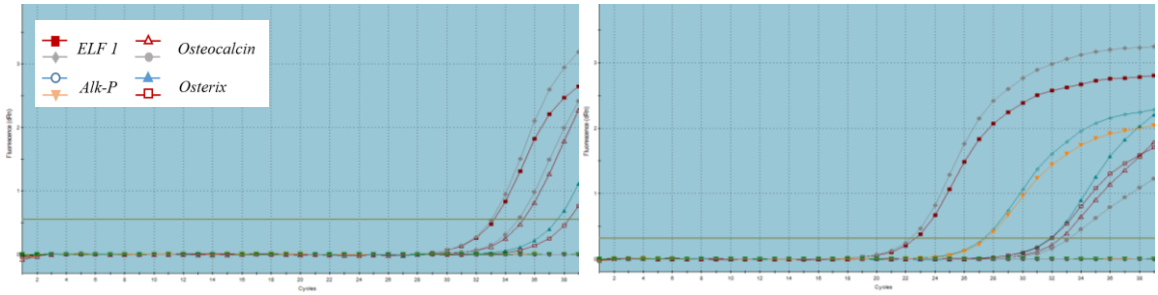

Figure 3.9 PCR amplification plots for osteogenesis studies. Fluorescence (dRn) on the y-axis versus amplification cycle on the x-axis for AF cells cultured under normal conditions (control) (left) and AF cells cultured under osteogenic media (left). Control AF appeared to have a small expression of osteocalcin, while being negative on the remaining markers. Osteogenic AF had distinct peaks for most of the osteogenic markers.

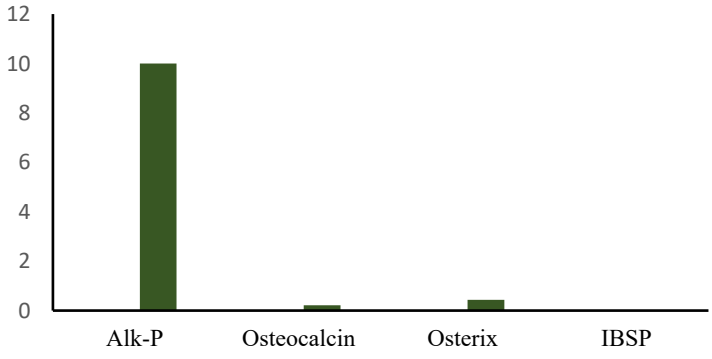

Figure 3.10 Gene expression of osteogenesis studies. AF cells cultured in osteogenic media showed positive expression of *Alk-P, Osteocalcin* and *Osterix* after three weeks. Alkaline phosphatase expression was increased compared to the rest of the genes. Control AF cells, cultured in IVD media were negative for osteogenic markers.

Osteogenic marker expression was positive for the AF cells that underwent osteogenesis studies. As seen in **Figure 3.10** alkaline phosphatase activity was significantly higher than that of osteocalcin and osterix, while IBSP did not give any distinct Ct values and was hence considered to not be expressed.

CHAPTER 4: DISCUSSION

4.1 Scaffold Characterization

Results from SEM imaging indicated that polycaprolactone scaffolds dissolved in HFIP demonstrated superiority in their characteristics compared to the ones dissolved in DCM. Some of the criteria that were used for the comparison were the diameter of the fibers, absence of beads and uniformity of fibers across the scaffolds. The fiber diameter and uniformity in electrospun scaffolds has proven to possess an important role for tissue engineered constructs bearing cells, affecting cellular attachment, proliferation, as well as cell-cell and cell-ECM interactions[54-57]. Chen et al. (2007), studied the relationship between fiber diameter and cellular adhesion as well as growth kinetics utilizing electrospun polycaprolactone scaffolds of different fiber diameters and seeding them with fibroblasts[54]. The study concluded that increasing the fiber diameter in uniform scaffolds, lead to a decrease in cellular attachment and proliferation[54]. Exception to that rule was the presence of beads in scaffolds consisting of very low viscosity polymeric solution and fiber diameters in the 100nm scale, which did not support cell adherence[54]. In this study PCL/HFIP scaffolds were chosen as optimal due to their increased uniformity of fiber morphology throughout the different polymer concentrations. Furthermore, it was believed that absence of beads and consistent, small fiber diameter would promote better attachment of the cells and hence better viability.

As it is depicted in **Figure 3.1**, PCL in DCM yielded scaffolds with great variation of fiber diameters and in some instances presented bead formation. On the other hand, PCL/HFIP scaffolds were uniform, with fiber diameters following a normal distribution (**Figures 3.1, 3.3**). In the case of the PCL/HFIP scaffolds, the fiber diameter increased, as

the polymer concentration increased, with significant difference between the 12% and the 20% (**Figure 3.2**). Previous literature shows that scaffolds with nanoscale features enhance cell adhesion and proliferation compared to constructs with larger fibers[54-57]. Laurencin et al. (1999) suggested that cellular organization is better around fibers with smaller diameters than those of the cells[58]. Current studies add to that, that nanoscale fibers play a role in the conformation of adhesion proteins (such as fibronectin) that later affect the adhesion profiles of the scaffolds[54]. Namely, smaller-fiber scaffolds adsorb more adhesion proteins that later increase the focal adhesion sites available for cells[54]. With that in mind, scaffolds with smaller fibers were preferred in this research.

Despite PCL/DCM scaffolds having some fibers smaller than those in PCL/HFIP constructs, the big range of their diameters and the formation of beads rendered them unsuitable for the purposes of this study. Such variations in fiber diameters could occur due to incomplete dissolution of polymer in the solvent, or during the electrospinning process, when the polymer solution jet is unstable[59]. Scaffolds that possess beads and are not uniform have decreased adherence of cells and minimal growth kinetics, as previously discussed in the study of Chen et al (2007). Due to the low surface area-to volume ratio, availability of substrate for the cells to attach is minimized[54]. Moreover, with the formation of beads, cell behavior on scaffolds is not consistent among the population, which renders it hard to explore the behavior of the cells and maintain good homeostasis of the scaffolded cells. Here PCL/HFIP scaffolds of 12% were used; this specific concentration was chosen over the 15% (despite them not having significant difference in their fiber diameters, as shown in **Figure 3.2**), due to the fact that they require less polymer and the dissolution times for the PCL in HFIP are reduced compared to more concentrated solutions.

The PCL scaffolds showed great potential as cell carriers, by possessing both biocompatibility and increased ability to adhere cells. As shown in **Figure 3.4**, fluorescently tagged MIAMI cells appeared to attach onto the scaffolds well, with a significant increase in adherence with increasing time of scaffold pre-incubation with culture media. PCL is a synthetic, biocompatible polymer that when degraded, it produces non-toxic byproducts, making it an ideal candidate for use in tissue engineering applications[68]. However, its hydrophobic character leads to poor interactions with cells[68]. Hence, to promote cell attachment, PCL scaffolds were incubated with culture media for a prolonged time, to allow adsorption of the media and creation of an environment that sustains cell viability. Seeding of GFP tagged MIAMI cells on scaffolds pre-treated with culture media for only 30 minutes, lead to cells "slipping off" the scaffolds and attaching on the surrounding plates instead (data not shown). When the scaffolds sufficiently absorbed the media, the cells attached on the scaffolds (**Figure 3.4B-C**). It is noticeable that MIAMI cells present on the scaffolds possessed different phenotypes compared to the ones attached on the plates, which was suggested to be due to the random orientation of the PCL fibers. Cells tended to follow the direction of the fibers, creating more elongated shapes, something that agreed with previous observations[33]. **Figure 3.4B** also indicates that the cells penetrated within the scaffolds, as well as attaching on their surfaces. GFP expression appeared to be blurry under different microscope focusing planes, which indicated that the cells were present in different depths of the scaffold and not only the surface. Cell adherence on and migration in the scaffolds is crucial to create biomimetic scaffolds with 3D architecture.

It is very important for tissue engineered constructs that are targeted for implantation, to consist of materials that are degradable, to allow for native cell infiltration, as well as replacement and regeneration of the tissue. However, in this study, scaffold degradation studies were not performed, due to the nature of the PCL polymer to resist degradation. Generally, polycaprolactone appears to degrade slowly, with data showing mass retention up to 6 both *in vitro* and *in vivo*[60]. Lam et al., (2008) studied the degradation pattern of PCL both *in vitro,* in PBS, and *in vivo* in a rabbit model and followed up their degradation patterns for up to 6 months[61]. They observed a maximum loss of 1% for the *in vitro* group and 7% for the *in vivo* one, with almost no changes in the mass or molecular weight of the polymer scaffold after the 6-month period[60]. Moreover, in their preliminary studies of a 2-year implantation of PCL and PCL-based scaffolds in critical-sized rabbit calvarial defect sites, Lam et al., (2008) observed long-term biocompatibility and late molecular weight decreases[60-61]. Here, since the IVD was the site of focus, it was decided that the late degradation and long-term viability of the scaffolds would allow for better mechanical support in the spine, and would deliver a better long-term solution for the regeneration of the disc.

4.2 Co-culture Studies and Troubleshooting

Reverse-transcription polymerase chain reaction or else RT-PCR is the most sensitive method to amplify and detect RNA targets (especially mRNA) and compare data from different samples and conditions[65]. Even though widely used in research nowadays, RT-PCR has introduced many challenges by requiring extreme optimization to avoid some

pitfalls. As it was observed in this research, PCR results can vary greatly and give rise to false-positives or negatives by a plethora of parameters.

This research was focused on RNA, which is the transcriptome of the cells. Unlike the DNA, which is the genome, transcriptome detection is highly dependent on context, which implies that expression level of RNA in cells (and specifically mRNA) can vary with physiology, pathology and/or development of the cells[66]. All these render the information contained within the RNA highly flexible and variable[66]. RT-PCR on its end is a complicated procedure on its own, consisting of extraction and isolation of RNA, reverse-transcription of the target RNA into cDNA and ultimately amplification and detection of the target template. These steps call for variations depending on the kits used and conditions followed and are highly susceptible to attenuation. Three main ways to group inhibitors of the PCR are inhibitors that 1) interfere with the lysis and RNA extraction, 2) degrade or capture nucleic acids and 3) inhibit the polymerase activity affecting the amplification of the target[66].

Initially, interference at the lysis level can occur when nucleases get added into the samples either by contact of the samples with contaminated equipment (pipettes, tubes and solutions that are not DNase/RNase-free) or by uncontrollable lysis. Some lysates can disturb the RNA if the appropriate protocol is not followed precisely. Interference with the extraction of RNA would be apparent during the quantification of the isolated samples, in which case RNA would not be present. In this experiment, TRIzol reagent was used, which is harsh on the cells but has nucleic acid protective abilities. Moreover, quantification with a NanoDrop spectrophotometer allowed for the determination of intact RNA and proved that RNA was not accidentally lysed. Hence, no inhibition due to lysis occurred.

Other than inhibition of the isolation step, another crucial issue in the PCR process is the quality of the RNA sample obtained. Samples that contain organic or inorganic contaminants, such as phenol residues can affect downstream processes in the reverse-transcription and amplification of the cDNA[65]. To determine the purity of the samples, the 260/280 and 260/230 absorbance ratios are important. Values larger than 1.8 for these ratios appear in samples that are free of DNA, proteins and organic contaminants. In this experiment, all samples selected had 260/280 ratios >1.8. However, samples used in the AF lineage studies and particularly the ones from cells seeded on scaffolds appeared to have very low 260/230 ratios. This meant that samples were not free of organic compounds. Following the exact protocol for samples without the scaffolds yielded good 260/230 ratio values. This, in combination with the fact that scaffolds were dissolved in the TRIzol to allow for cells to detach could implicate that residues from the PCL scaffolds could be responsible for variability in the results during PCR. Despite using reverse-transcription and PCR kits that minimize effect of organic contaminants from phenol in the downstream applications, contamination from organic residues of the scaffold might require additional protection from inhibition.

In this protocol, non-specific reverse transcription was performed to synthesize target cDNAs. During this process, complementary DNA templates are produced, without specific primers to the target. Namely, an amount of random primers allows for the collection of the most amount of DNA possible. Despite yielding a bigger amount of DNA, the product of the reverse transcription contains more than one type of cDNA transcript (since it transcribes all present RNA in the cells) and not just that of the target. In the case of low amounts of target RNA, most of the concluding cDNA is derived from ribosomal

RNA (not mRNA that shows the appropriate protein expression). Utilization of specific primers for reverse transcription would be more expensive and would require extensive analysis of the transcriptome of both the AF and MIAMI cells used, but it could focus the cDNA to the target one wanted.

As mentioned previously, PCR can be inhibited in various ways. Another way is because of the fact that different templates have varying amplification probabilities and efficiencies[65]. Some samples even have specific dilution thresholds, meaning that diluting them more could lead to great amplification variations and hence faulty readings[65].

Additionally, to that, the quality of the primers used for the targeted detection of specific genes is very important. Primers that are not precise to the DNA template (with differences going down to one base pair) can terminate the primer extension after the annealing and can lead to false-negative readings[65]. Thus, primer design needs to be careful and validated properly. In the case of this experiment, porcine primers were designed and used that were previously described[64]. To validate the specificity of the primers to the target templates, Basic Local Alignment Search Tool (BLAST) (NCBI, NIH) was used as previously described[67]. Some of the samples did not appear to have great specification and that could explain why there were no results for targets for *Col 2, Oct-4* and *Nanog.* Modifying the primers into more specific ones could lead to more distinct results in the future.

Housekeeping genes, are genes that are universally found in specific cell populations and are used to normalize data that do not necessarily possess the same amounts of nucleic acid. The selection of housekeeping genes must be validated properly to determine that particular cells do indeed express the housekeeping gene and in

appropriate amounts. Here, *ELF-1α* was used to normalize the data in the PCR. However, despite showing appropriate expression in samples that underwent osteogenesis, *ELF-1α* did not have a consistent expression in the samples containing plain AF and/or MIAMI cells, with Ct values ranging from 23-32 units. This observation and the fact that the expression was not stable (differences between replicates), could indicate *ELF-1α* to not be the optimal housekeeping gene in this case. PCR analysis using different and/or multiple housekeeping genes could be performed to better determine the expression of AF-, MIAMI-only and co-cultured cells.

4.3 Osteogenesis Studies

Annulus fibrosus cells were used in this study as the cells to drive the differentiation of the multipotent MIAMI cells. AF cells were chosen, because they are native in the IVD and because they are already differentiated, which would mean they could lead to differentiation of MIAMI cells without getting affected in the process. However, it has been previously shown that under different conditions, rabbit AF-derived cells can be induced to differentiate into osteocytes, chondrocytes and adipocytes[53]. In that study, Liu et al. (2014) showed that there is a population of AF-derived stem cell-like cells that can differentiate into the aforementioned lineages, when placed in osteogenic, chondrogenic and adipogenic media[53].

Porcine AF cells were cultured in this research in osteogenic media, to examine the possibility of these cells to differentiate into other, possibly unwanted lineages. Osteogenesis was chosen as an experiment here, due to the fact that osteocytes can create

calcifications on the scaffolds that could affect the viability and phenotype of the seeded cells and the functionality of the scaffolds altogether, on the long run.

Despite keeping similar phenotype under the microscope, after three weeks of culturing cells in the osteogenic conditions had small expression of alkaline phosphatase, as determined by histology (**Figure 3.5, Figure 3.6**). Moreover, PCR confirmed these data and showed that other markers are getting upregulated after three weeks, in small amounts (**Figure 3.9, Figure 3.10**). Particularly, alkaline phosphatase was present in high-fold compared to *Osterix* and *Osteocalcin*, which indicated starting levels of calcification/osteogenesis[68]. *Alk-P* promotes mineralization, which is the initial step to calcification in pre-bone tissues[68]. *Osteocalcin* and *Osterix* are both markers of osteoblast differentiation, which in case here was in very early stages. Longer incubation of the AF cells could lead to increased expression of the remainder of the markers and could have led to changes in the phenotypes of the cells. Altogether, these results showed that AF cells could get affected by their environment and be induced to differentiate, which could lead to calcifications of the scaffolds and variations with the phenotypes in the co-cultures. Further studies *in vitro* and *in vivo* would be required to determine what exactly these conditions are and how potential differentiation of the co-cultured stem cells.

4.4 Study Limitations and Future Studies

One of the main limitations of the study, was the creation of randomly oriented scaffolds. It was previously proven that scaffolds having parallel fiber alignment possess superior properties than the ones with random orientation. Particularly, mimicking the native tissue, parallel fibers create lamination that is essential in the mechanics of the AF.

To be able to create AF with aligned fibers, modifications in the electrospinning apparatus would have to be accustomed. In the future, studies involving a high spinning rotator as the collector, instead of the aluminum covered, glass slide, would allow for the fabrication of scaffolds with parallel, aligned fiber morphologies, which could yield superior construct characteristics[32,33].

Another limitation of the study was the selection of the cells. Pigs have been shown to be an efficient animal model for IVD tissue engineering. However, with the use of human disc and MIAMI cells, the study could approach closer clinical trials. Additionally, porcine and human MIAMI cells could possess different surface antigens, which implies that further discriminations between the animal model and the humans are present and should be studied before making any conclusions.

Finally, mechanical testing is essential for disc tissue engineering and fabrication of biomimetic, synthetic scaffolds. As mentioned previously in this report, IVD is crucial for the mechanics of the spine, withstanding the compression forces of the body, functioning as a shock absorbent and allowing for bending, twisting and other movements of the everyday life. Although it was shown in various publications that aligned, electrospun PCL scaffolds approach the tensile strength range required in native annulus fibrosus tissue, mechanical tests of the proposed AF/MIAMI constructs would give a better idea on whether or not these scaffolds could be promising in the future for clinical trials.

Future studies will also involve the optimization of the process for the collection of the transcriptome, to determine if the co-cultures indeed provide the wanted results. Extraction of cells from the PCL scaffolds will be studied, as to avoid contamination from scaffold or phenol residues in the samples. Even though other nucleic acid extraction kits

have been tested previously to TRIzol and were deemed unsuccessful in RNA isolation from the proposed constructs, further techniques will be evaluated. Additionally, new primers and housekeeping genes will be studied in addition to running more housekeeping genes for optimization of the normalization procedure.

4.5 Conclusion

MIAMI cells are very promising for applications in the tissue engineering. Being a sub-population of MSCs they possess more embryonic-like stem cell markers and have been shown to proliferate in a plethora of lineages. IVD tissue engineering could thus use them as substitutes to native cell or MSC implantation. Although observations and distinct conclusions have been hindered in this research, due to variations in the PCR readings, it has been previously shown that electrospun scaffolds can be used to house co-cultures of native AF cells and stem cells to allow for creation of tissue engineering constructs for replacement of degenerative discs[10]. Here it was shown that co-cultures of AF and MIAMI cells expressed increased *Col 1* compared to MIAMI-only controls, which could indicate differentiation of the latter ones into AF-lineages. Moreover, this research showed that there are AF-derived cells that can differentiate, which could be a concern in *in vivo* studies with this proposed platform. Further optimizations in the process are required, however, the proposed platform could be improved for uses in IVD tissue engineering.

REFERENCES

1. Raj, P. Prithvi. "Intervertebral disc: anatomy-physiology-pathophysiology-treatment" *Pain Practice* 8.1 (2008): 18-44.

2. Adams, Michael A., and Peter J. Roughley. "What is intervertebral disc degeneration, and what causes it?" *Spine* 31.18 (2006): 2151-2161.

3. Whatley, Benjamin R., and Xuejun Wen. "Intervertebral disc (IVD): structure, degeneration, repair and regeneration." *Materials Science and Engineering: C* 32.2 (2012): 61-77.

4. Silva-Correia, Joanna et al. "Tissue engineering strategies applied in the regeneration of the human intervertebral disk." *Biotechnology Advances* 31.8 (2013): 1514-531.

5. Wagner, Diane R., and Jeffrey C. Lotz. "Theoretical model and experimental results for the nonlinear elastic behavior of human annulus fibrosus." *Journal of Orthopaedic Research* 22.4 (2004): 901-909.

6. Luo, Xuemei, et al. "Estimates and patterns of direct health care expenditures among individuals with back pain in the United States." *Spine* 29.1 (2004): 79-86.

7. Vadalà, Gianluca, et al. "Intervertebral disc regeneration: from the degenerative cascade to molecular therapy and tissue engineering." *Journal of Tissue Engineering and Regenerative Medicine* 9.6 (2015): 679-690.

8. Xu, Baoshan, et al. "Intervertebral disc tissue engineering with natural extracellular matrix-derived biphasic composite scaffolds." *PloS one* 10.4 (2015): e0124774.

9. Wan, Yuqing, et al. "Biphasic scaffold for annulus fibrosus tissue regeneration." *Biomaterials* 29.6 (2008): 643-652.

10. Tsai, Tsung-Lin, et al. "Intervertebral disc and stem cells co-cultured in biomimetic extracellular matrix stimulated by cyclic compression in perfusion bioreactor." *The Spine Journal* 14.9 (2014): 2127-2140.

11. Vadalà, Gianluca, et al. "Bioactive electrospun scaffold for annulus fibrosus repair and regeneration." *European Spine Journal* 21.1 (2012): 20-26.

12. Resnick, Daniel K., and William C. Watters. "Lumbar disc arthroplasty: a critical review." *Clinical Neurosurgery* 54 (2007): 83.

13. Kurtz, Steven M., et al. "Polyethylene wear and rim fracture in total disc arthroplasty." *The Spine Journal* 7.1 (2007): 12-21.

14. Alini, Mauro, et al. "The potential and limitations of a cell-seeded collagen/hyaluronan scaffold to engineer an intervertebral disc-like matrix." *Spine* 28.5 (2003): 446-453.

15. Hubert, Mark G., et al. "Gene therapy for the treatment of degenerative disk disease." *Journal of the American Academy of Orthopaedic Surgeons* 16.6 (2008): 312-319.

16. Vadala, Gianluca, et al. "Coculture of bone marrow mesenchymal stem cells and nucleus pulposus cells modulate gene expression profile without cell fusion." *Spine* 33.8 (2008): 870-876.

17. Richardson, Stephen M., et al. "The differentiation of bone marrow mesenchymal stem cells into chondrocyte-like cells on poly-L-lactic acid (PLLA) scaffolds." *Biomaterials* 27.22 (2006): 4069-4078.

18. Wilke, Hans-Joachim, et al. "Is a collagen scaffold for a tissue engineered nucleus replacement capable of restoring disc height and stability in an animal model?" *European Spine Journal* 15.3 (2006): 433-438.

19. Sakai, Daisuke, et al. "Transplantation of mesenchymal stem cells embedded in Atelocollagen® gel to the intervertebral disc: a potential therapeutic model for disc degeneration." *Biomaterials* 24.20 (2003): 3531-3541.

20. Chang, G., et al. "Porous silk scaffolds can be used for tissue engineering annulus fibrosus." *European Spine Journal* 16.11 (2007): 1848-1857.

21. Leone, Gemma, et al. "Amidic alginate hydrogel for nucleus pulposus replacement." *Journal of Biomedical Materials Research Part A* 84.2 (2008): 391-401.

22. Dang, Jiyoung M., et al. "Temperature-responsive hydroxybutyl chitosan for the culture of mesenchymal stem cells and intervertebral disk cells." *Biomaterials* 27.3 (2006): 406-418.

23. Saad, L., and M. Spector. "Effects of collagen type on the behavior of adult canine annulus fibrosus cells in collagen–glycosaminoglycan scaffolds." *Journal of Biomedical Materials Research Part A* 71.2 (2004): 233-241.

24. Park, Sang-Hyug, et al. "Intervertebral disk tissue engineering using biphasic silk composite scaffolds." *Tissue Engineering Part A* 18.5-6 (2011): 447-458

25. Le Visage, Catherine, et al. "Interaction of human mesenchymal stem cells with disc cells: changes in extracellular matrix biosynthesis." *Spine* 31.18 (2006): 2036-2042.

26. Di Martino, Alberto, et al. "Chitosan: a versatile biopolymer for orthopaedic tissue-engineering." *Biomaterials* 26.30 (2005): 5983-5990.

27. Strassburg, Sandra, et al. "Co-culture induces mesenchymal stem cell differentiation and modulation of the degenerate human nucleus pulposus cell phenotype." *Regenerative Medicine* 5.5 (2010): 701-711.

28. Lu, Z. F., et al. "Differentiation of adipose stem cells by nucleus pulposus cells: configuration effect." *Biochemical and Biophysical Research Communications* 359.4 (2007): 991-996.

29. Tapp, Hazel, et al. "Adipose-derived mesenchymal stem cells from the sand rat: transforming growth factor beta and 3D co-culture with human disc cells stimulate proteoglycan and collagen type I rich extracellular matrix." *Arthritis Research & Therapy* 10.4 (2008): R89.

30. Nomura T, et al. "Nucleus pulposus allograft retards intervertebral disc degeneration." *Clinical Orthopaedics and Related Research* 389 (2001):94–101.

31. Liu, Chen, et al. "The effect of the fiber orientation of electrospun scaffolds on the matrix production of rabbit annulus fibrosus-derived stem cells." *Bone Research* 3 (2015): 15012.

32. Lazebnik, Mihael, et al. "Biomimetic method for combining the nucleus pulposus and annulus fibrosus for intervertebral disc tissue engineering." *Journal of Tissue Engineering and Regenerative Medicine* 5.8 (2011): e179-e187.

33. Koepsell, Laura, et al. "Tissue engineering of annulus fibrosus using electrospun fibrous scaffolds with aligned polycaprolactone fibers." *Journal of Biomedical Materials Research Part A* 99.4 (2011): 564-575.

34. Nesti, Leon J., et al. "Intervertebral disc tissue engineering using a novel hyaluronic acid–nanofibrous scaffold (HANFS) amalgam." *Tissue Engineering Part A* 14.9 (2008): 1527-537.

35. Nerurkar, Nandan L., et al. "Engineered disc-like angle-ply structures for intervertebral disc replacement." *Spine* 35.8 (2010): 867.

36. Li, Wan-Ju, et al. "Electrospun nanofibrous structure: a novel scaffold for tissue engineering." *Journal of Biomedical Materials Research* 60.4 (2002): 613-621.

37. Bhardwaj, Nandana, and Subhas C. Kundu. "Electrospinning: a fascinating fiber fabrication technique." *Biotechnology Advances* 28.3 (2010): 325-347.

38. Lannutti, J., et al. "Electrospinning for tissue engineering scaffolds." *Materials Science and Engineering: C* 27.3 (2006): 504-509.

39. Urban, Jill PG, et al. "Nutrition of the intervertebral disc." *Spine* 29.23 (2004): 2700-2709.

40. D'Ippolito, Gianluca, et al. "Marrow-isolated adult multilineage inducible (MIAMI) cells, a unique population of postnatal young and old human cells with extensive expansion and differentiation potential." *Journal of Cell Science* 117.14 (2004): 2971-2981.

41. Young, Randell G., et al. "Use of mesenchymal stem cells in a collagen matrix for Achilles tendon repair." *Journal of Orthopaedic Research* 16.4 (1998): 406-413.

42. Pittenger, Mark F., et al. "Multilineage potential of adult human mesenchymal stem cells." S*cience* 284.5411 (1999): 143-147.

43. Conget, Paulette A., and José J. Minguell. "Phenotypical and functional properties of human bone marrow mesenchymal progenitor cells." *Journal of Cellular Physiology* 181.1 (1999): 67-73.

44. D'Ippolito, Gianluca, et al. "Age-related osteogenic potential of mesenchymal stromal stem cells from human vertebral bone marrow." *Journal of Bone and Mineral Research* 14.7 (1999): 1115-1122.

45. Colter, David C., et al. "Rapid expansion of recycling stem cells in cultures of plastic-adherent cells from human bone marrow." *Proceedings of the National Academy of Sciences* 97.7 (2000): 3213-3218.

46. Colter, David C., et al. "Identification of a subpopulation of rapidly self-renewing and multipotential adult stem cells in colonies of human marrow stromal cells." *Proceedings of the National Academy of Sciences* 98.14 (2001): 7841-7845.

47. Reyes, Morayma, et al. "Purification and ex vivo expansion of postnatal human marrow mesodermal progenitor cells." *Blood* 98.9 (2001): 2615-2625.

48. Gronthos, Stan, et al. "Molecular and cellular characterization of highly purified stromal stem cells derived from human bone marrow." *Journal of Cell Science* 116.9 (2003): 1827-1835.

49. Rahnemai-Azar, Amirali, et al. "Human marrow-isolated adult multilineage-inducible (MIAMI) cells protect against peripheral vascular ischemia in a mouse model." *Cytotherapy* 13.2 (2011): 179-192.

50. D'Ippolito, Gianluca, et al. "Low oxygen tension inhibits osteogenic differentiation and enhances stemness of human MIAMI cells." *Bone* 39.3 (2006): 513-522.

51. J-R Delcroix, Gaëtan, et al. "Multi-layered scaffold to mimic hyaline articular cartilage architecture." *Current Tissue Engineering* 5.1 (2016): 21-28.

52. Schneider, C.A., et al. "NIH Image to ImageJ: 25 years of image analysis". *Nature Methods* 9, 671-675, 2012.

53. Liu, Chen, et al. "Identification of rabbit annulus fibrosus-derived stem cells". *PLoS One* 9.9 (2014): e108239.

54. Chen, Ming, et al. "Role of fiber diameter in adhesion and proliferation of NIH 3T3 fibroblast on electrospun polycaprolactone scaffolds." *Tissue Engineering* 13.3 (2007): 579-587.

55. Thapa, Anil, et al. "Polymers with nano-dimensional surface features enhance bladder smooth muscle cell adhesion." *Journal of Biomedical Materials Research Part A* 67.4 (2003): 1374-1383.

56. Miller, Derick C., et al. "Mechanism (s) of increased vascular cell adhesion on nanostructured poly (lactic-co-glycolic acid) films." *Journal of Biomedical Materials Research Part A* 73.4 (2005): 476-484.

57. Thapa, Anil, et al. "Nano-structured polymers enhance bladder smooth muscle cell function." *Biomaterials* 24.17 (2003): 2915-2926.

58. Laurencin, Cato T., et al. "Tissue engineering: orthopedic applications." *Annual Review of Biomedical Engineering* 1.1 (1999): 19-46.

59. Deitzel, Joseph M., et al. "The effect of processing variables on the morphology of electrospun nanofibers and textiles." *Polymer* 42.1 (2001): 261-272.

60. Lam, Christopher XF, et al. "Evaluation of polycaprolactone scaffold degradation for 6 months in vitro and in vivo." *Journal of Biomedical Materials Research Part A* 90.3 (2009): 906-919.

61. Lam, Christopher XF, et al. "Dynamics of in vitro polymer degradation of polycaprolactone-based scaffolds: accelerated versus simulated physiological conditions." *Biomedical Materials*3.3 (2008): 034108.

62. Granéli, Cecilia, et al. "Novel markers of osteogenic and adipogenic differentiation of human bone marrow stromal cells identified using a quantitative proteomics approach." *Stem Cell Research* 12.1 (2014): 153-165.

63. Monjo, Marta, et al. "In vivo expression of osteogenic markers and bone mineral density at the surface of fluoride-modified titanium implants." *Biomaterials* 29.28 (2008): 3771-3780.

64. D'Ippolito, Gianluca, et al. "Isolation and characterization of swine MIAMI cells: a valuable animal model for adult stem cell therapy." *Cell* 2.5 (2014): e1215.

65. Bustin, Stephen A., and Tania Nolan. "Pitfalls of quantitative real-time reverse-transcription polymerase chain reaction." *Journal of Biomolecular Techniques: JBT* 15.3 (2004): 155.

66. Wilson, I. G. "Inhibition and facilitation of nucleic acid amplification." *Applied and Environmental Microbiology* 63.10 (1997): 3741.

67. Altschul, Stephen F., et al. "Basic local alignment search tool." *Journal of Molecular Biology* 215.3 (1990): 403-410.

68. Orimo, H. "The mechanism of mineralization and the role of alkaline phosphatase in health and disease." *Journal of Nippon Medical School* 77.1 (2010): 4-12.

69. Zander, Nicole E., et al. "Quantification of protein incorporated into electrospun polycaprolactone tissue engineering scaffolds." *ACS Applied Materials & Interfaces* 4.4 (2012): 2074-2081.